Max-Planck-Institut für Plasmaphysik

Nuclear Fusion
Modeling and validation of energetic particle slowing down on Wendelstein 7-X

Samuel A. Lazerson

HELMHOLTZ RESEARCH FOR GRAND CHALLENGES

MAX PLANCK GESELLSCHAFT

EUROfusion

This work has been carried out within the framework of the EUROfusion Consortium and has received funding from the Euratom research and training programme 2014-2018 and 2019-2020 under grant agreement No 633053. The views and opinions expressed herein do not necessarily reflect those of the European Commission.

Modeling and validation of energetic particle slowing down on Wendelstein 7-X

Samuel A. Lazerson[1], David Pfefferlé[2], Michael Drevlak[1], Håkan Smith[1], Simppa Äkäslompolo[3], Pavlos Xanthopoulos[1], Oliver Ford[1], Paul McNeely[1], Norbert Rust[1], Sergey Bozhenkov [1], Dirk Hartmann[1], Robert C. Wolf[1] and the W7-X Team

[1]Max-Planck-Institut für Plasmaphysik, 17491 Greifswald, Germany

[2]University of Western Australia, 6009 Crawley, Australia

[3]Aalto University, 02150 Espoo, Finland

Abstract

The energetic particle slowing down model in the BEAMS3D stellarator neutral beam code is validated against analytic models and experimental data from the Wendelstein 7-X experiment (W7-X). Recently, the first neutral beam experiments in W7-X have been performed providing validation of neutral beam deposition codes. This work builds upon that work, following the gyrocenter orbits of the neutral beam generated fast ions to the plasma boundary. A discharge solely heated by neutral beam injection is used to compare neoclassical heat flux estimates to neutral beam fueling, heating and current drive. Ion heat fluxes for the discharge are found to closely match neoclassical estimates while a shortfall of electron heat flux is found. Experimental estimates of electron heat diffusivity suggest that electron turbulence has been destabilized by density peaking in the discharge. Neutral beam current drive dominates over the bootstrap current resulting in a reversal in toroidal current as seen in experiment. Heat flux associated with lost fast ions is presented. The effect of magnetic configuration and density on such such parameters is also assessed. Benchmarking with analytic estimates and other energetic particle codes is presented.

What does this paper address?

- Multi-code orbit following comparisons
- Benchmarking of slowing down operators for fast ions
- Effect on magnetic configuration on orbits
- Simulations of pure NBI discharge (20181009.43)
  - Fueling
  - Heat deposition
  - Neutral Beam Current Drive
  - Particle Losses (not wall loads)
- Effect of density and magnetic configuration on these quantities

Neutral Beam Deposition addressed in

Lazerson, S. A. *et al.* (2020). Validation of the BEAMS3D neutral beam deposition model on Wendelstein 7-X. *Nuclear Fusion*. http://doi.org/10.1088/1741-4326/ab8e61

Wall Loads will be addressed in future work.

Multi-code NBI deposition validation on W7-X published

- **Full 3D Equilibrium Reconstruction with STELLOPT**
  - **Thomson, XICS, CXRS, ECE, Magnetics, Interferometer**
- **Cross-code benchmark shows good agreement**
- **Comparison with beam attenuation validates code**

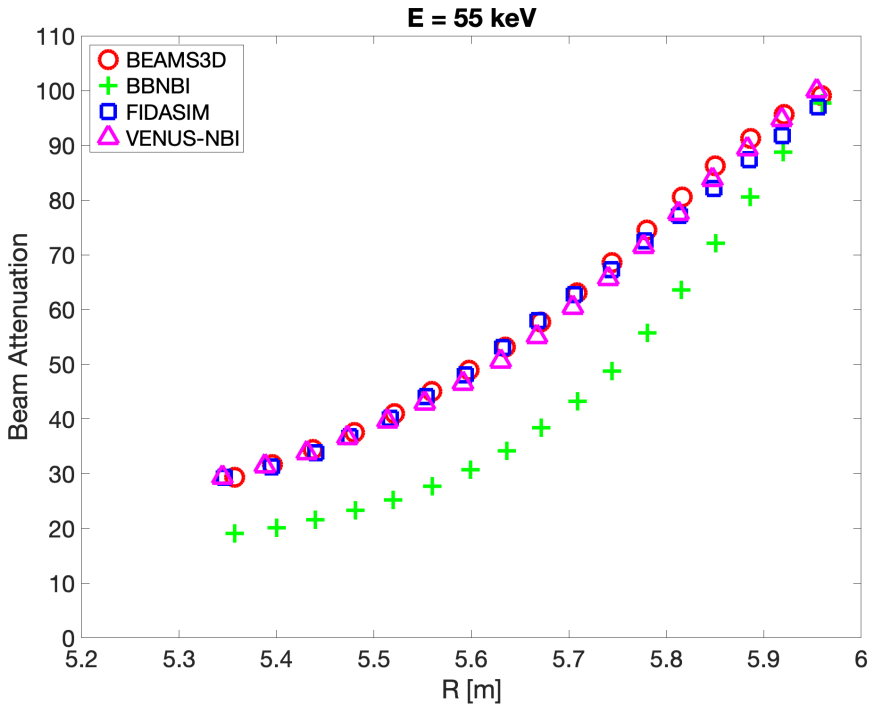

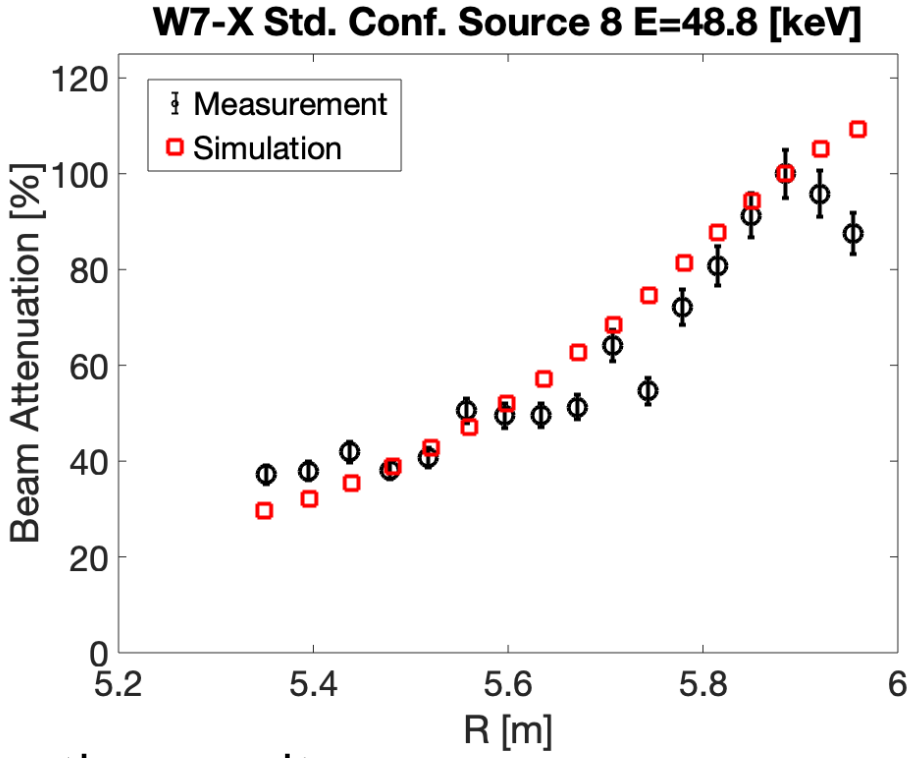

This work builds on these results

Lazerson, et al. Nuclear Fusion (https://doi.org/10.1088/1741-4326/ab8e61)

Introduction to the W7-X Neutral Beam System

- One of two boxes operated in OP1.2b
  - 2 of 4 Sources
  - 1.7 MW, 55 kV H2
  - 5 s discharge (focus)

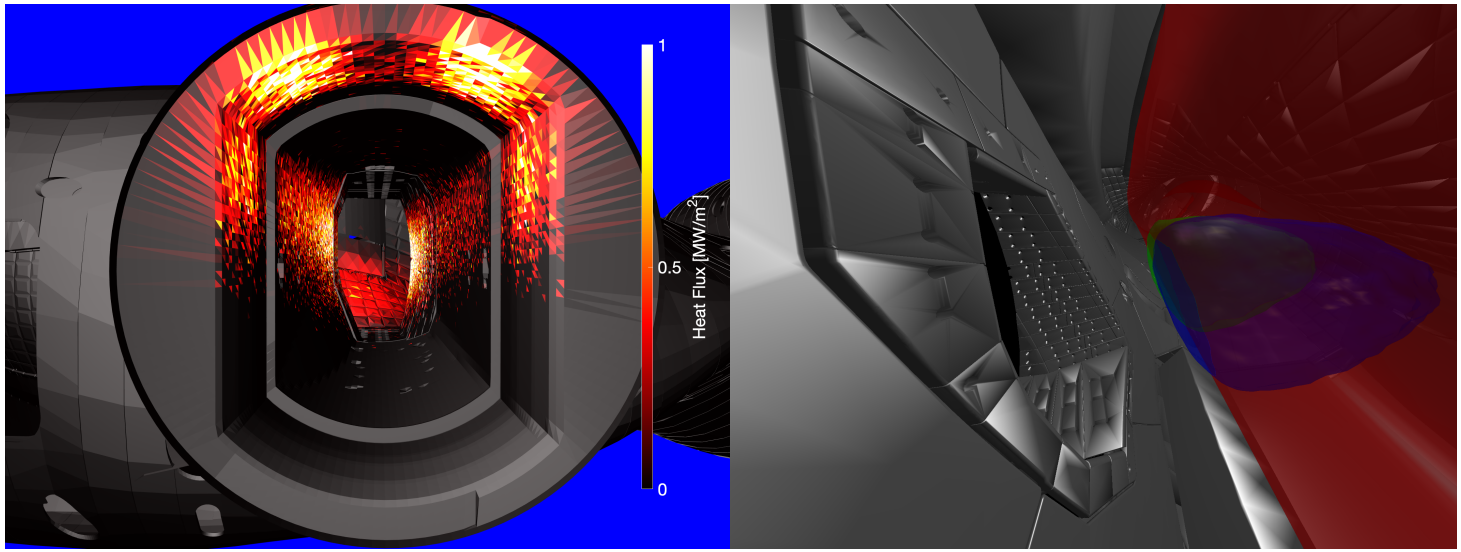

Figure 1. Neutral beam geometry showing port interaction (left) and ionization clouds (right). The equilibrium last closed magnetic flux surface has been visualized in red, while the clouds of ionized particles from source 7 (green) and source 8 (blue) are depicted.

BEAMS3D Benchmarked against other codes

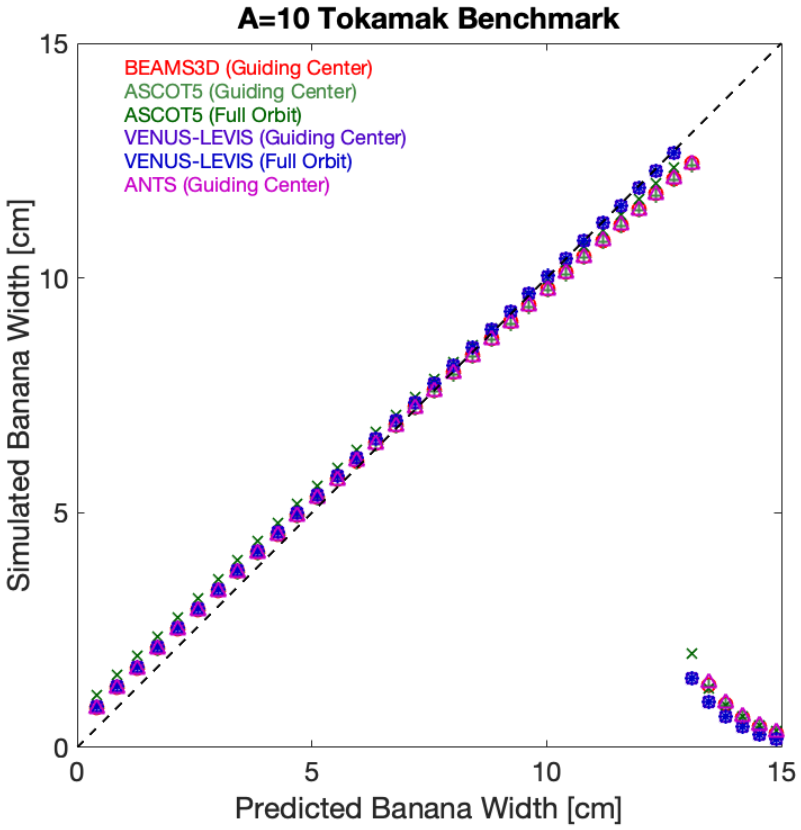

Figure 2. Comparison of simulated banana orbit width to analytic estimates for a variety of codes and particle models. An aspect ratio 10 circular cross section tokamak equilibrium is used in these simulations and orbits are collisionless.

- Bannan Orbit widths benchmarked
  - Large aspect ratio
  - Circular cross-section tokamak

BEAMS3D Equations

$$\frac{d\vec{R}}{dt} = \frac{\hat{b}}{qB} \times \left(\mu \nabla B + \frac{m v_{\parallel}^2}{B} (\hat{b} \cdot \nabla) \vec{B} \right) + v_{\parallel} \hat{b} + \frac{\vec{E} \times \vec{B}}{B^2}$$

$$\frac{dv_{\parallel}}{dt} = -\frac{\mu}{m} \hat{b} \cdot (\nabla B)$$

Radial Electric Field and ASCOT5 interface are new features

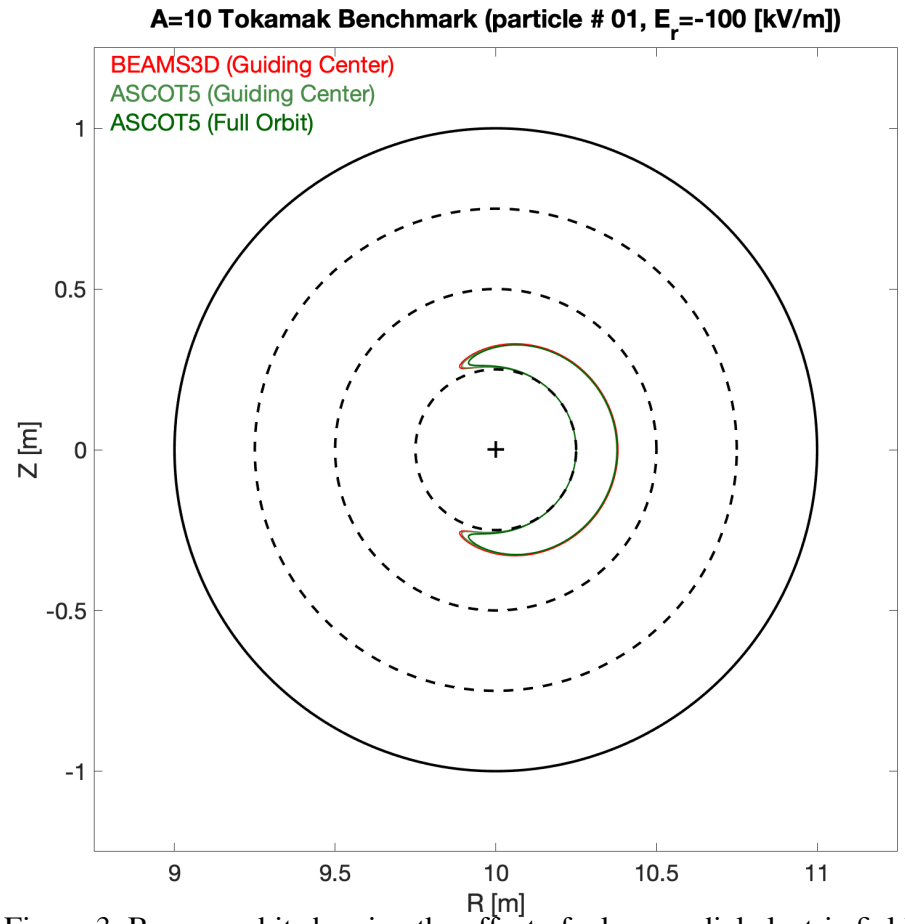

Figure 3. Banana orbit showing the effect of a large radial electric field widening the orbit.

- BEASM3D used to create ASCOT5 Input
  - Magnetic Fields
    - VMEC (others)
    - Coils
    - MGRID
  - Plasma Profiles
  - Particle Birth
  - Wall
- Electric field a new feature of BEAMS3D

In this work we wish to validated our slowing down simulations for BEAMS3D

Energy lost by fast ions is gained by plasma.
Particles thermalize at 1.5x local ion thermal speed.

$$\frac{\partial < v >}{\partial t} = -\frac{v}{\tau_s} - \frac{v_c^3}{\tau_s v^2}$$

Electron

Ion

$$P(\zeta) = \frac{1}{\sqrt{2\pi}\sigma} \exp\left(-\frac{(\zeta - \langle\zeta\rangle)^2}{2\sigma^2}\right)$$

$$\langle\zeta\rangle = \zeta_0\left(1 - \frac{2v_s\Delta t}{v^3}\right) \qquad \sigma^2 = \frac{2v_s\Delta t}{v^3}(1 - \zeta_0^2)$$

$$\tau_s = \frac{m_i}{m_e}\frac{(4\pi\epsilon_0)^2}{4\sqrt{2\pi}}\frac{3\sqrt{m_e T_e^3}}{N_e Z_i^2 e^4 \ln\Lambda}$$

$$v_c = \left[\frac{3\sqrt{\pi}}{4}\frac{m_e}{m_i}\right]^{1/3} v_{T_e}$$

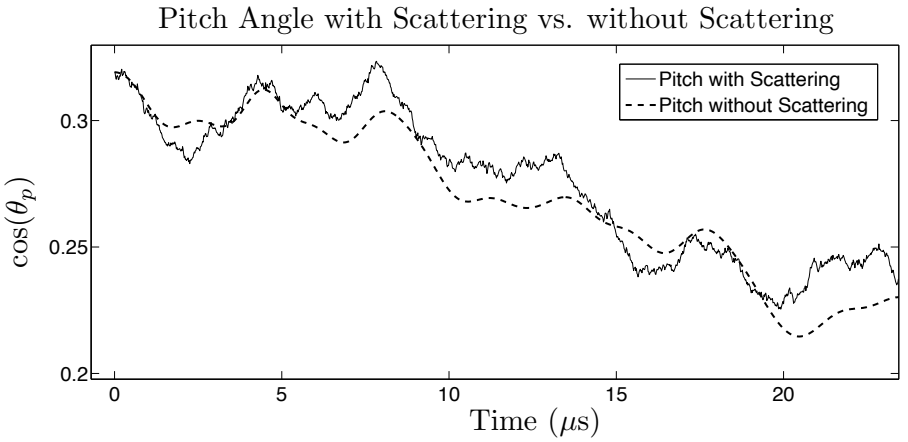

BEAMS3D Slowing down operator has been benchmarked

- Ion to electron heating depends on critical energy
- In agreement with theoretical estimates
- Allows for some validation of pitch angle operator as well

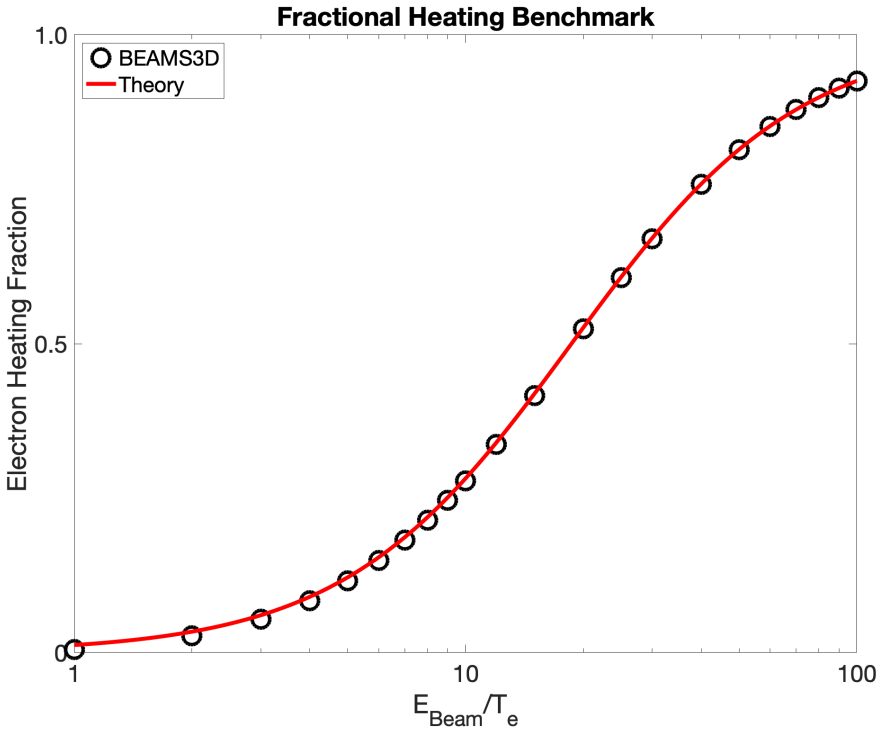

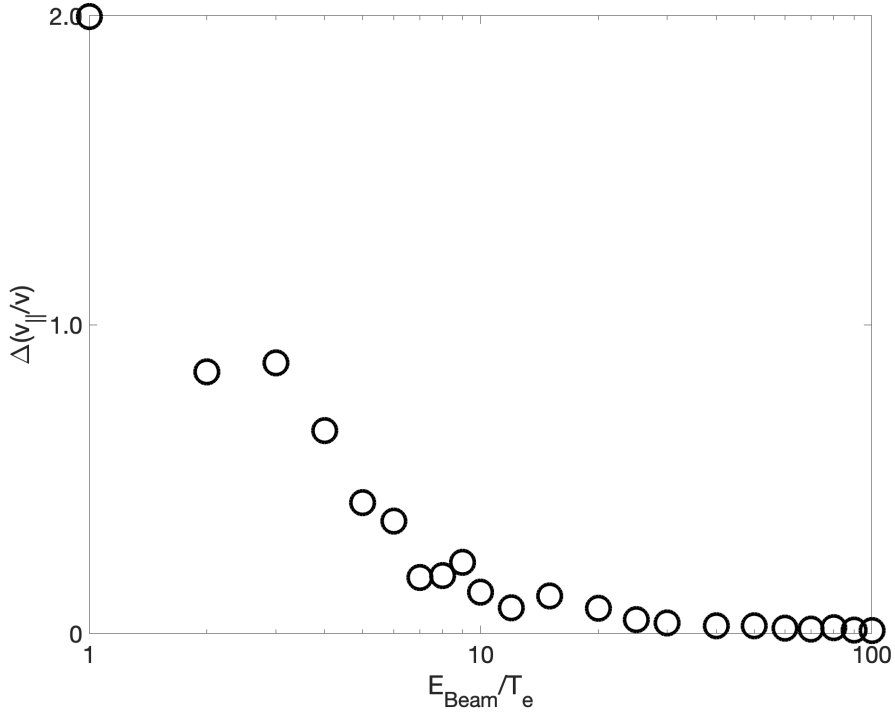

Figure 4. Fraction of power deposited to electrons as a function of the particle energy for a large aspect ratio tokamak (A=10). The plasma is chosen to have 1000 eV electron temperature and electron density of 1.2×10^{19} m^3.

Effect of pitch angle scattering operator.

A10TOK; 5° pitch; 50 particles; 1 ms; n_e=1.2E19 m^{-3}; T_e=1 keV; r/a=0.25; D_2

Overview of simulation results

- Set of configurations scanning density and magnetic configuration are considered
- The 5s NBI High Mirror shot is used for validation of profile quantities

Table 2. Overview of the BEAMS3D simulations results. Integrated powers rounded to the nearest 10 [kW] are displayed. All simulations based on two source with a combine neutral power of 3420 [kW]. All simulations account for 400 [kW] of power loss to the neutral beam duct. Discharge 20181009.43 indicates values average over 5 time slices.

Shot ID	Mag. Conf.	n_{e0} $[m^{-3}]$	Power [kW]			
			Born	Ion	Electron	Wall
20180812.12	Standard	6.37×10^{19}	2300	1020	1030	250
20180812.17	Standard	2.80×10^{19}	1400	570	370	460
20180812.19	Standard	11.3×10^{19}	2760	1010	1570	180
20180822.12	High Iota	5.82×10^{19}	2140	850	1070	220
20180823.20	High Mirror	7.39×10^{19}	2500	780	1490	230
20181009.43	High Mirror	$10.5 - 27.8 \times 10^{19}$	2820	860	1860	100

Magnetic field structure plays a role in orbits

- Standard, High Iota, and High mirror considered
  - High Iota has more local ripple wells
  - High mirror appears QPS-like

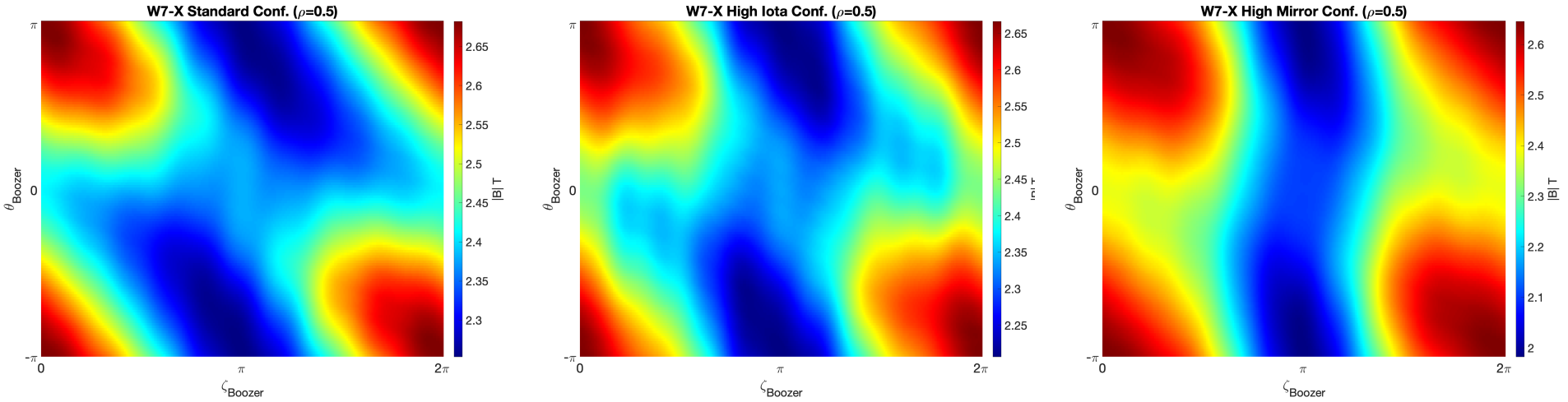

Figure 5. Magnetic field strength in Boozer magnetic coordinates for three magnetic configurations in W7-X. One field period is depicted at the mid radius ($\varrho = 0.5$). The poloidal angle $\theta_{Boozer} = 0$ is taken to be located on the outboard side.

Deeply trapped particles exhibit different trapping behavior

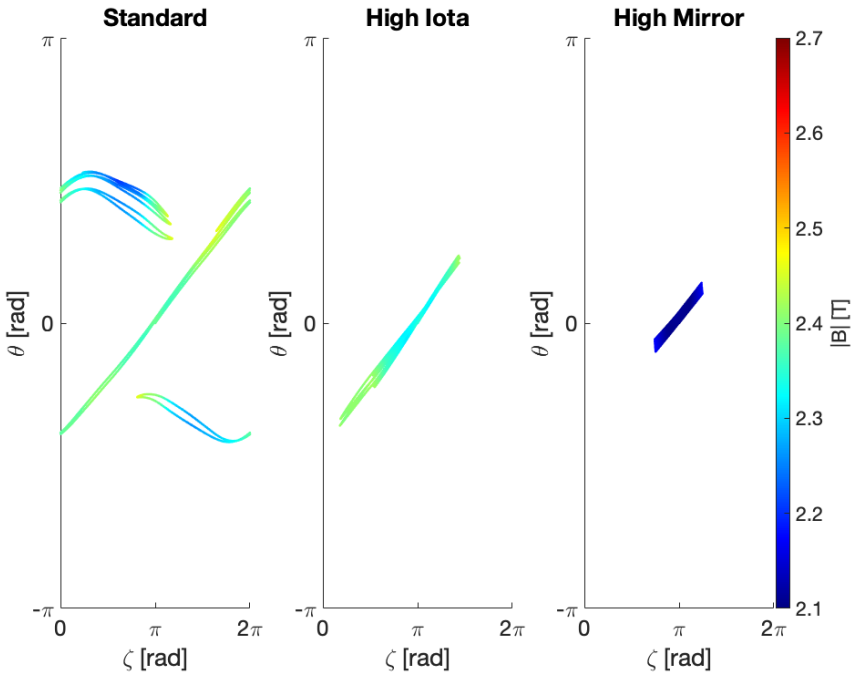

Figure 6. Trajectory for a deeply trapped (pitch angle 10° collisionless particle in W7-X. Particle is launched from outboard mid-plane in the triangular cross section. Color contours indicate local field strength.

- Standard Configuration shows trapping across multiple field periods
- High Iota has some ripple like loss behavior
- High mirror shows orbits drifting in poloidal direction.

Passing particles also have magnetic configuration dependence

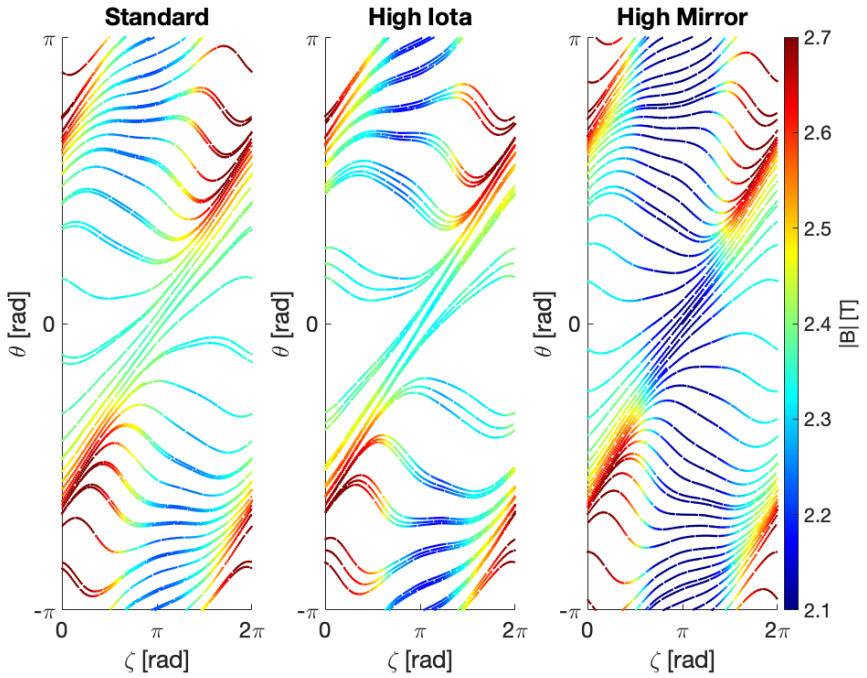

Figure 7. Trajectory for a passing (pitch angle 80°) collisionless particle in W7-X. Particle is launched from outboard mid-plane in the triangular cross section. Color contours indicate local field strength.

- Standard and High mirror show poloidal drift
- High iota appears to have exclusion regions
- Points to interplay between curvature and grad(B) drifts

Simulated fueling appears larger than experimental values

- Electron fueling based on beam birth
- Ion fueling based on thermalization of fast ions
- Discrepancy being assessed

$$\frac{\partial n_k}{\partial t} = -\nabla \cdot \Gamma_k + S_k$$

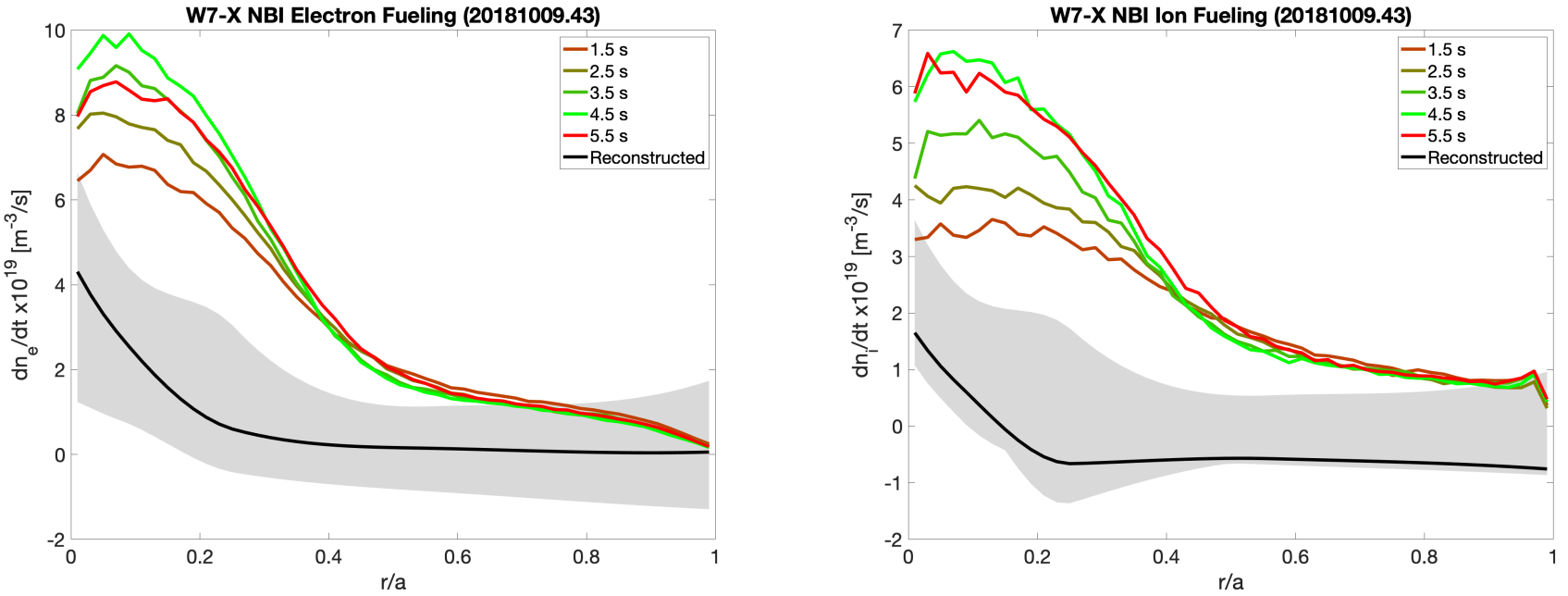

Figure 8. Electron (left) and ion (right) thermal density source terms for a purely NBI heated discharge in W7-X. The reconstructed density change is plotted by linearizing the density profile from 1.5 s to 5.5 s of the discharge. The shaded region depicts the range of possible values based on reconstructed profiles.

Analysis of energy transport significantly simplified in this shot

The energy transport equation for a species is written

$$\frac{3}{2}\frac{\partial n_k T_k}{\partial t} = -\frac{1}{V'}\frac{\partial}{\partial \rho}\left(V'\langle|\nabla\rho|\rangle Q_k\right) + P_k + P_{coll}^{\alpha/\beta}$$

which simplifies for steady state and Ti=Te

$$0 = \boxed{-\frac{1}{V'}\frac{\partial}{\partial \rho}\left(V'\langle|\nabla\rho|\rangle Q_k\right)} + \boxed{P_k}$$

Neoclassical BEASM3D

$$Q_k = \frac{\left\langle|\nabla\rho|^2\right\rangle}{\langle|\nabla\rho|\rangle}\chi_k n_k \frac{\partial T_k}{\partial \rho}$$

W7-X 20181009.43 NBI Only Discharge

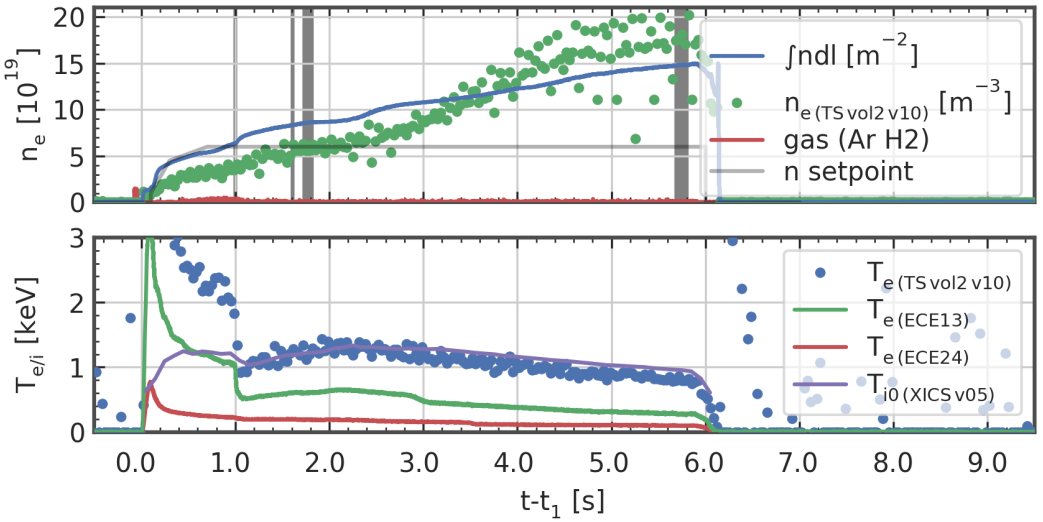

Ions temperature well described by Neoclassical transport

- Ion heat flux explained by neoclassical transport
- Electrons appear to be dominated by anomalous transport
  - Density peaking suggests TEM plays strong role in discharge

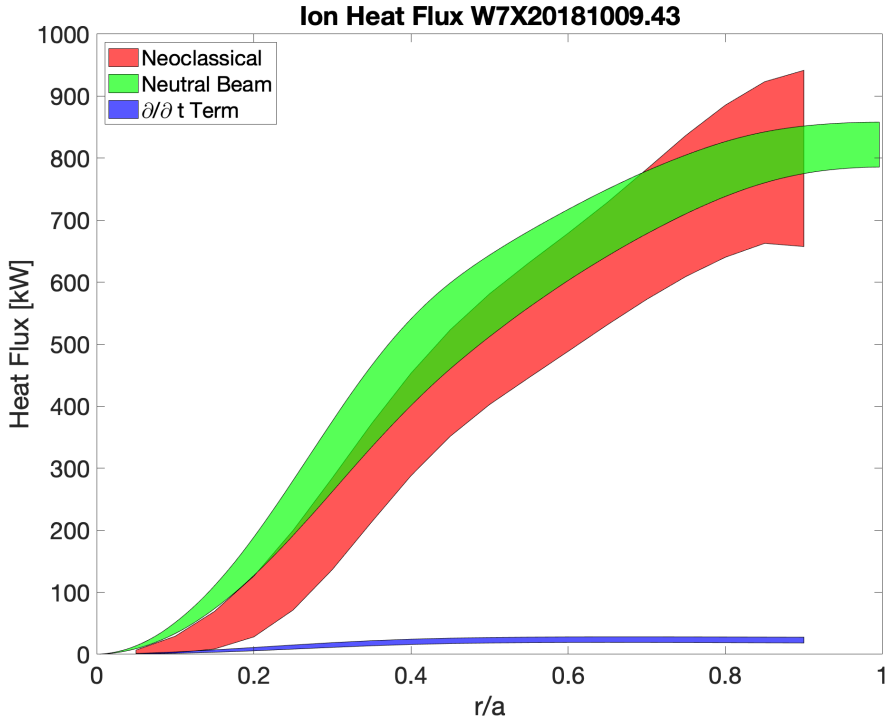

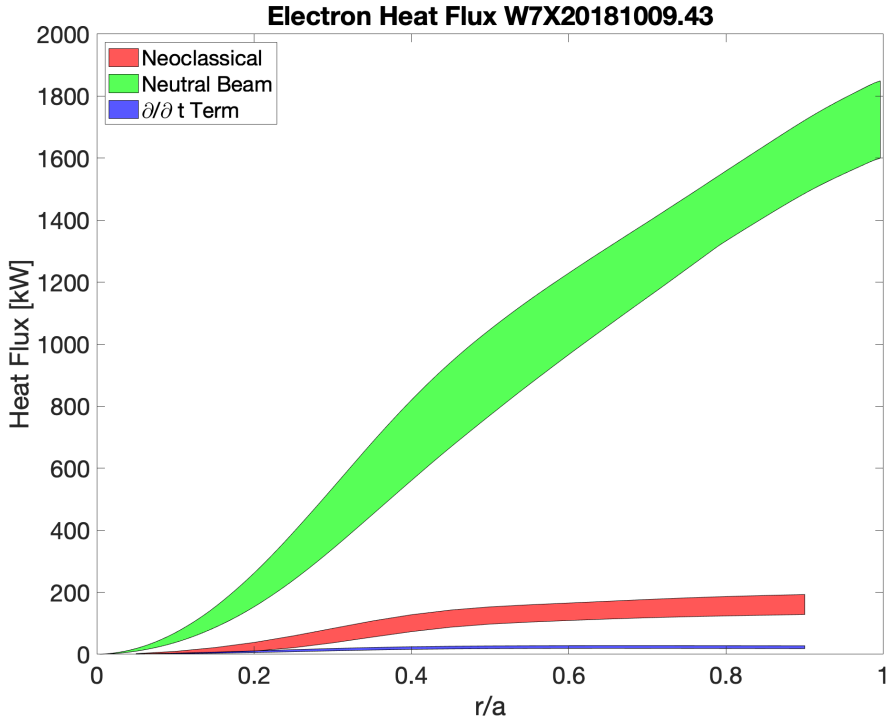

Figure 10. Comparison of transport terms for a discharge solely heated by NBI (20181009.43). Shaded regions indicate variation of discharge period. Neoclassical term calculated using the NEOTRANSP code, neutral beam term from BEAMS3D slowing down simulations, and time derivative term from experimental data.

Neutral Beam current drive calculated accounting for trapped electron correction.

The current density driven by the NBI system is derived from the fast ion current and a correction associated with trapped electrons.

$$j_{NBCD} = j_f \left[1 - \frac{Z_f}{Z_{eff}} (1 - G) \right]$$

where G can be taken to be the l31 Neoclassical coefficient. In the paper we calculate this with the Hirshman-Sigmar moment method

$$l_{31} = \frac{x \left[\left(0.754 + 2.21 Z_{eff} + Z_{eff}^2 \right) + x \left(0.348 + 1.243 Z_{eff} + Z_{eff}^2 \right) \right]}{1.414 Z_{eff} + Z_{eff}^2 + x \left(0.754 + 2.657 Z_{eff} + 2 Z_{eff}^2 \right) + x^2 \left(0.348 + 1.243 Z_{eff} + Z_{eff}^2 \right)}$$

$$x = f_{trapped} / (1 - f_{trapped}) \qquad f_{trapped} = 1 - \frac{3}{4} \frac{\langle B^2 \rangle}{B_{max}} \int_0^1 \frac{\lambda d\lambda}{\left\langle \sqrt{1 - \lambda B / B_{max}} \right\rangle}$$

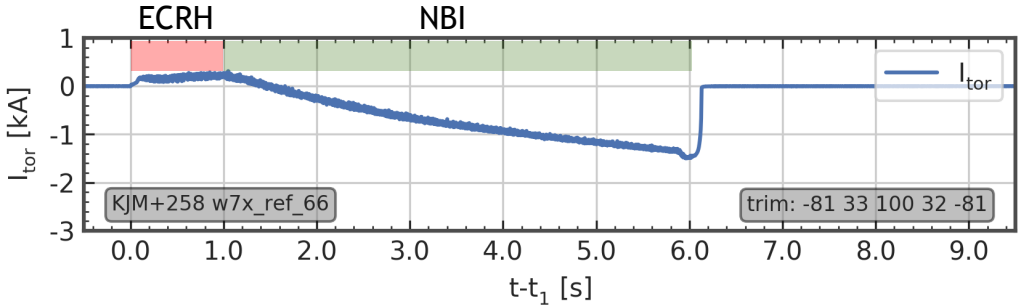

Neutral beam current drive predicts current direction reversal

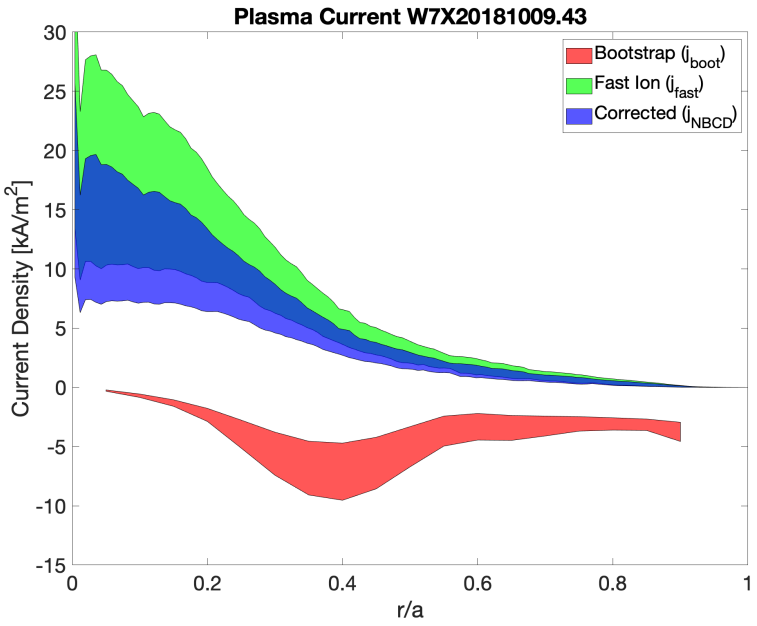

Figure 13. Bootstrap, fast ion and Ohkawa corrected neutral beam current densities for NBI-only discharge 20181009.43. Shaded regions indicate variation of profiles over 5 seconds of NBI operation. The neutral beam clearly drives current in the opposite direction to that of the bootstrap.

- Neoclassical and NBCD in opposite directions
- NBCD significantly larger than neoclassical value
- Experiments alternating sources confirm efficiency.

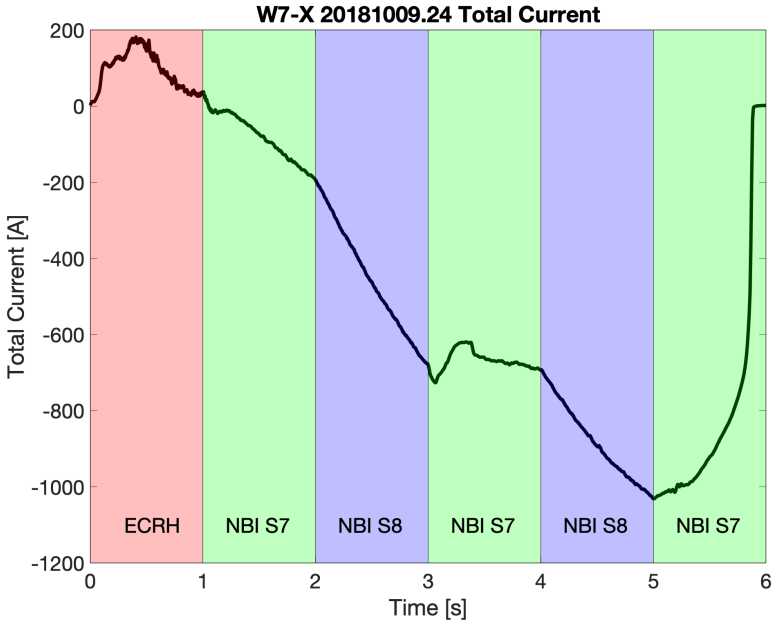

Loss structure shows asymmetries in wall loads

- **Particles were stopped at the VMEC last closed flux surface in this work**

Density [m3]	Peak Heat Flux [kW/m3]
3E+19	134
6E+19	101
1.1E+20	90

Configuration	Peak Heat Flux [kW/m3]
Standard	101
High Iota	126
High Mirror	83

Standard

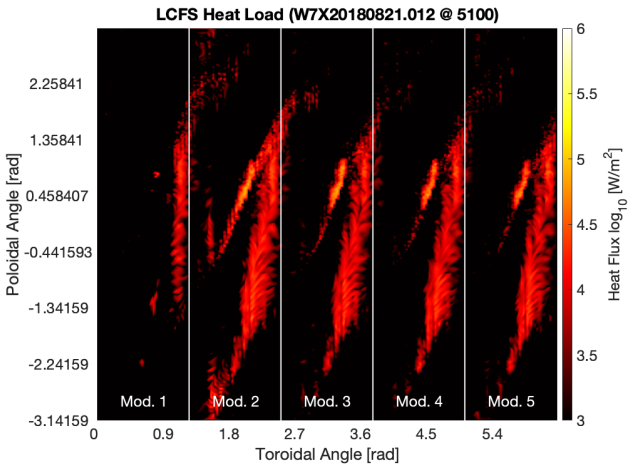

High Iota

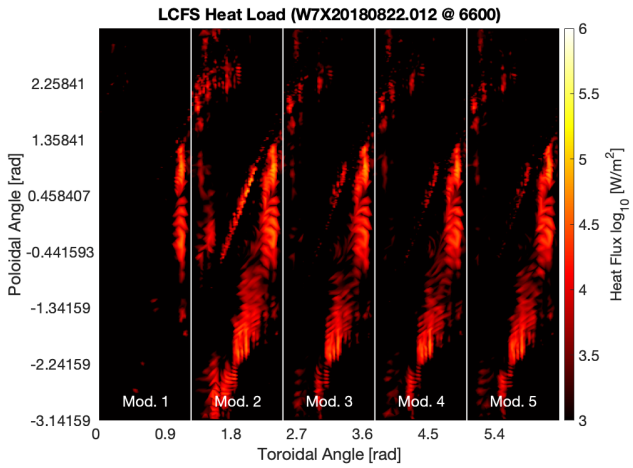

High Mirror

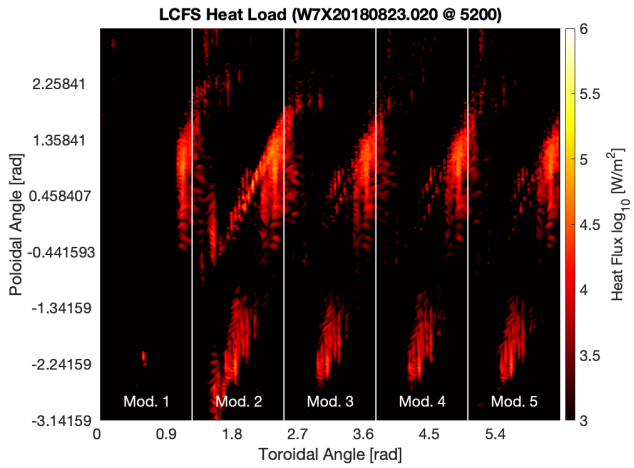

Figure 14. Heat flux through VMEC equilibrium boundary for the standard (left), high iota (center), and high mirror (right) magnetic configurations. In these plots $\theta = 0$ corresponds to the outboard mid-plan of the device. Similar maximum levels of heat flux are present between configurations while loss patterns vary somewhat.

Conclusions

- Multi-code benchmarking shows good agreement on toy model problem
- BEAMS3D slowing down operator has been validated against analytic model
- BEAMS3D Fueling estimates consistent with experiment
  - Validation requires more sophisticated experiments
- BEAMS3D ion heating quantitatively validated against W7-X data
  - Electron validation requires additional work
  - NBI discharge seems to be TEM dominated
- BEAMS3D current drive qualitatively validated
  - Quantitative validation requires current density profile reconstruction
- Validated deposition and slowing down results now allows quantitative work on wall load validation

Suzuki Model Implementation in BEAMS3D

- BEAMS3D previously used the PREACT implementation of ADAS for beam deposition.
- Suzuki et al. model has recently been implemented.
- Shows excellent agreement with ADAS for W7-X case

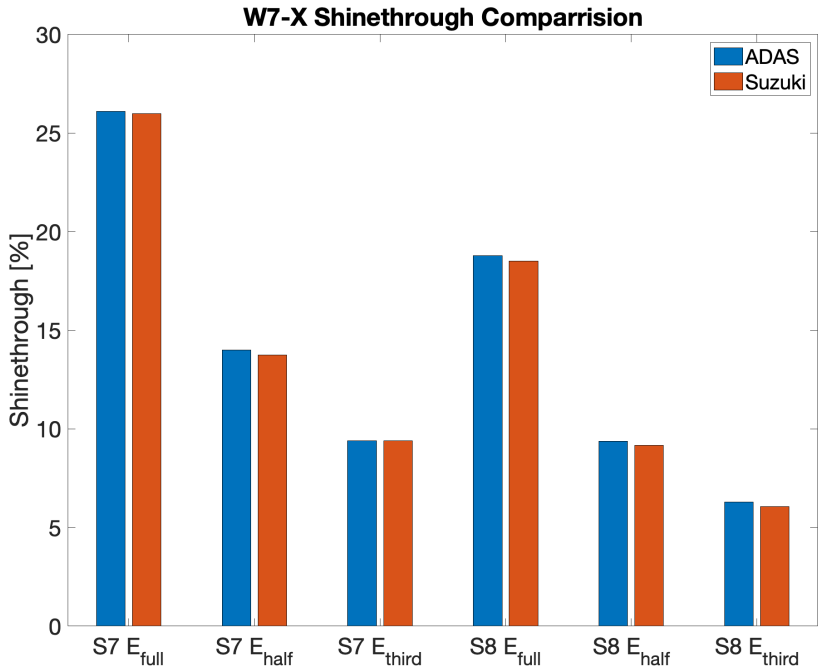

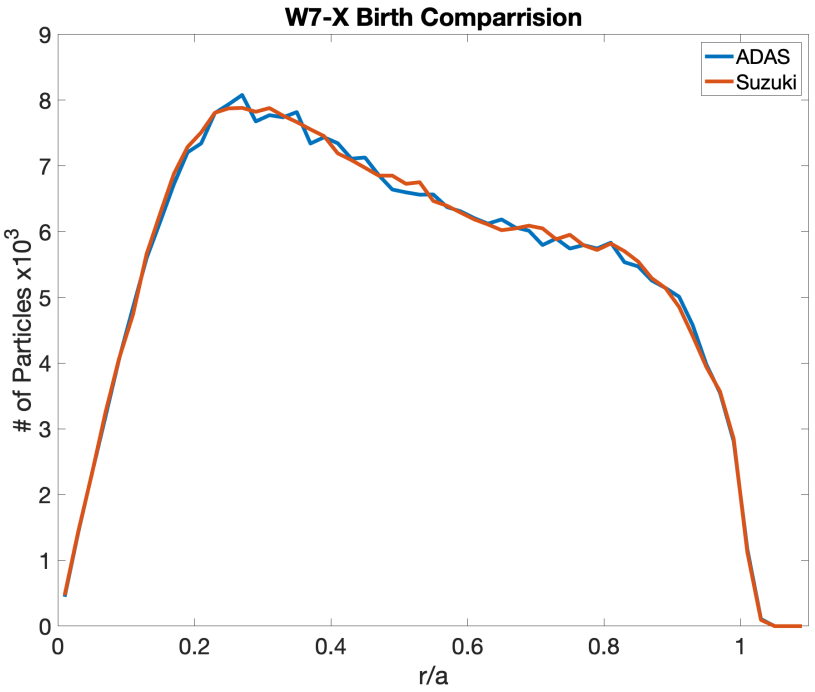

Suzuki, S., et al. (1999). PPCF, 40(12). http://doi.org/10.1088/0741-3335/40/12/009

Pure NBI discharge shows strong density peaking

- Density becomes strongly peaked
- Clear transition between core and edge density profiles

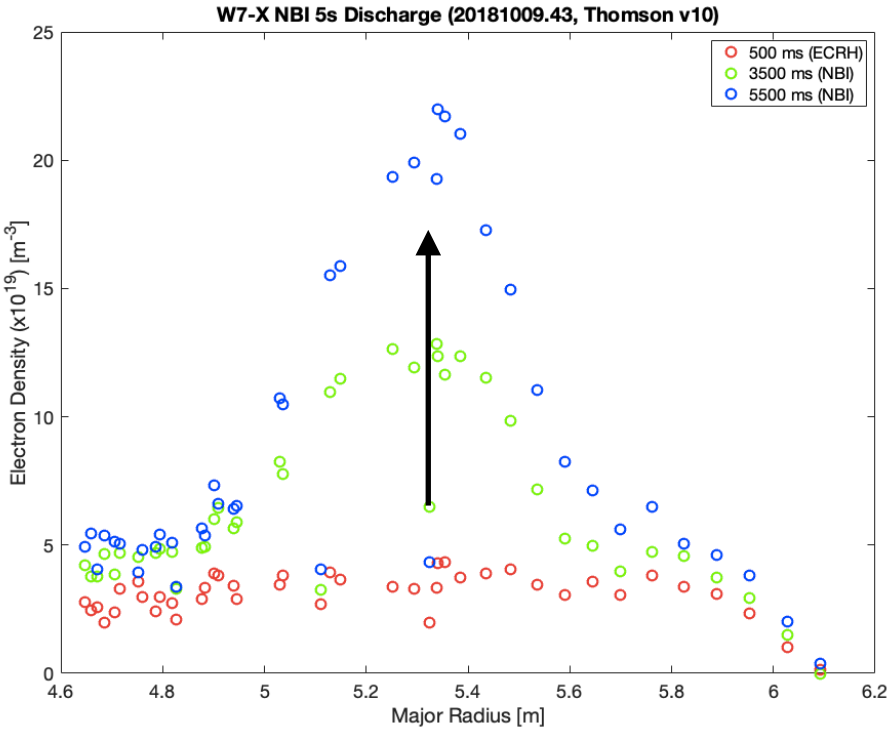

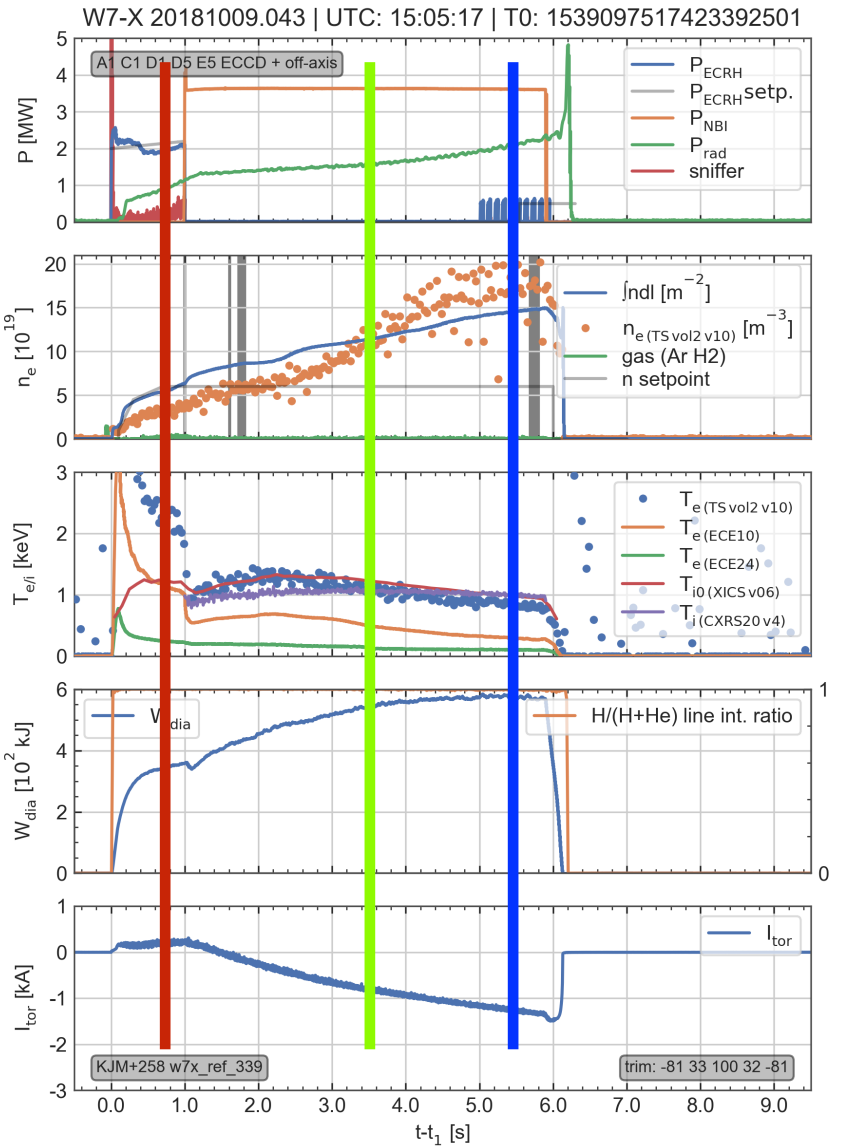

Addition of ECRH brings density control

- Strong gradient region remains
- Core density flattens
- Density rise arrested

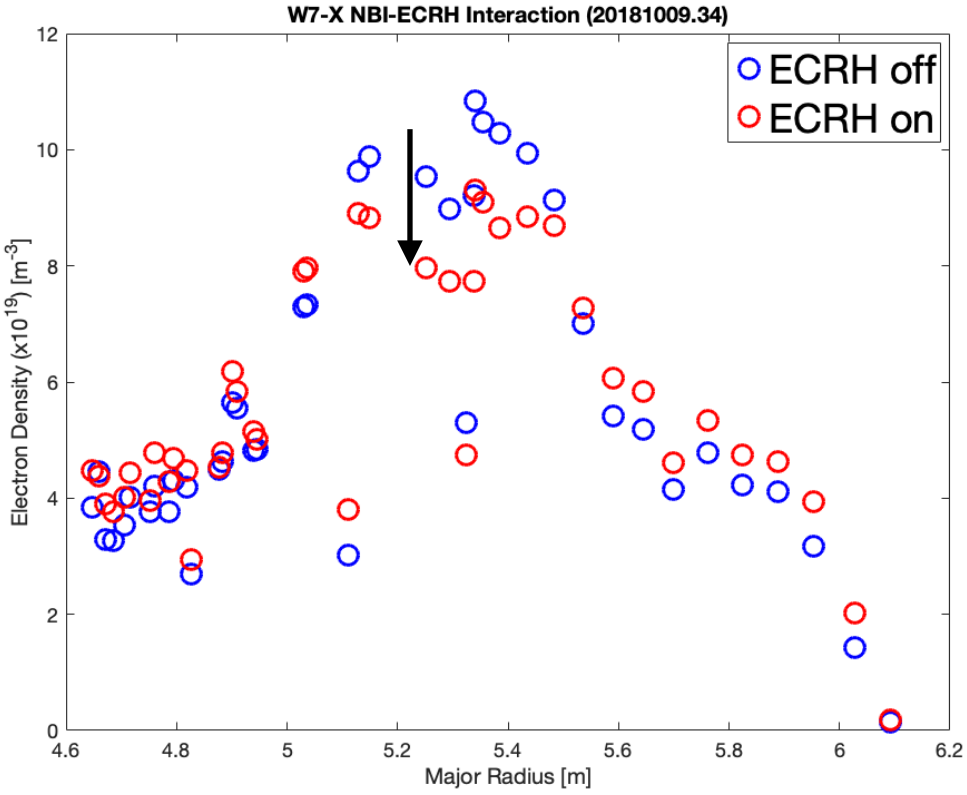

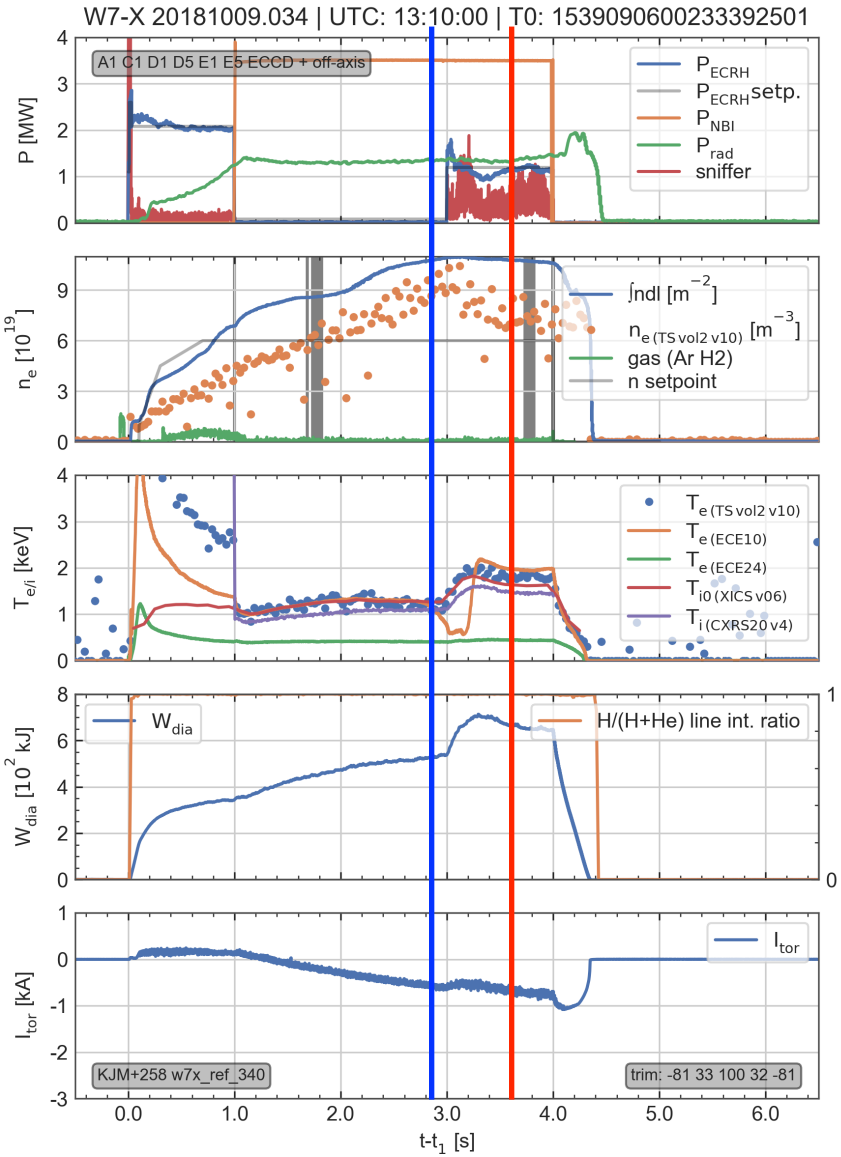

Comparison of collisionless orbits for W7-X underway

- W7-X standard configuration equilibrium used for benchmarking
  - 3 Radial positions and 7 pitches considered
  - Collision-less simulations compared
- Mostly good agreement with some outliers

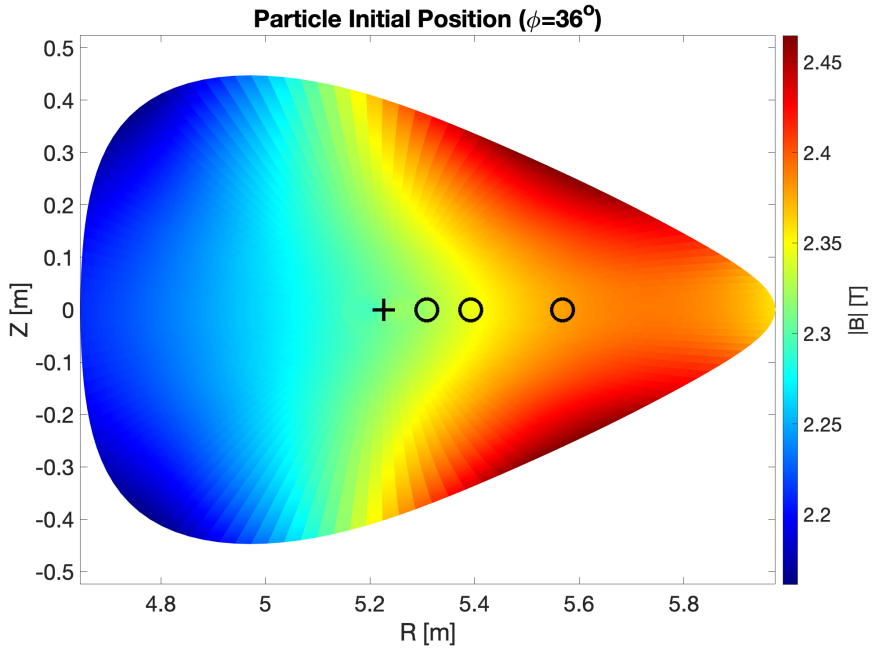

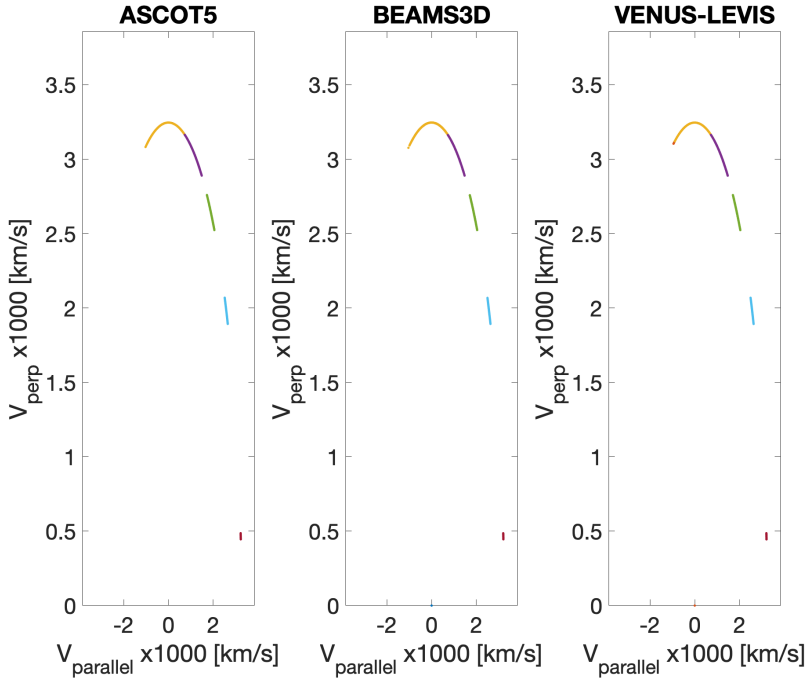

Deeply trapped particles can good agreement

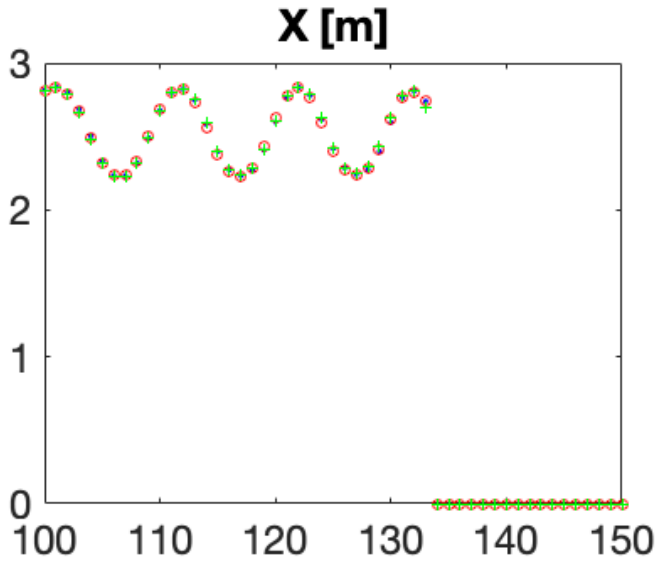

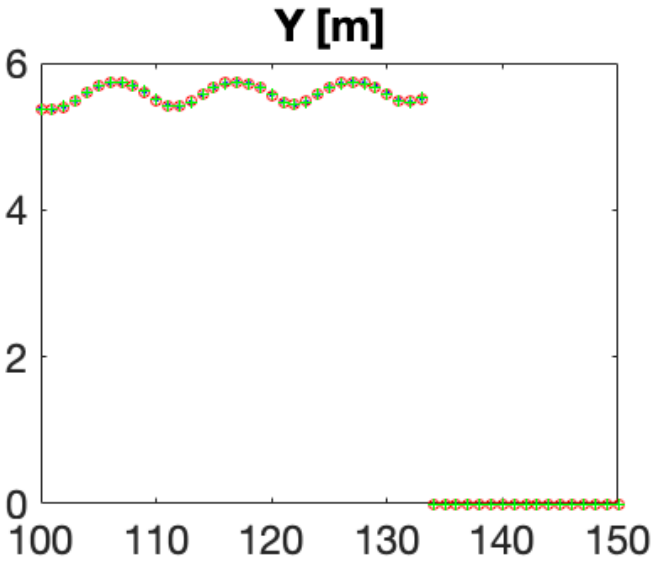

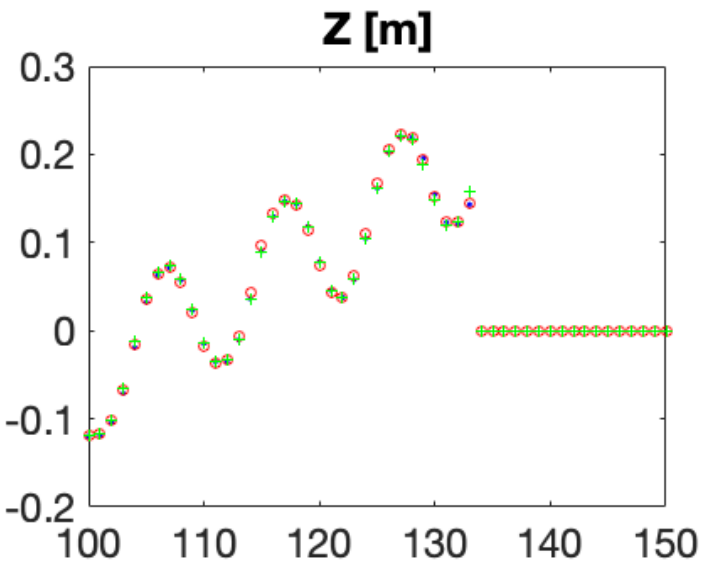

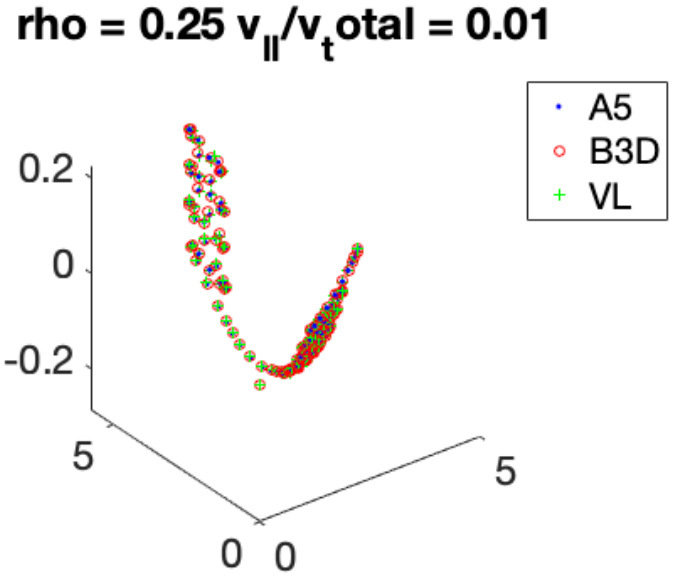

Deeply trapped particles can poor agreement

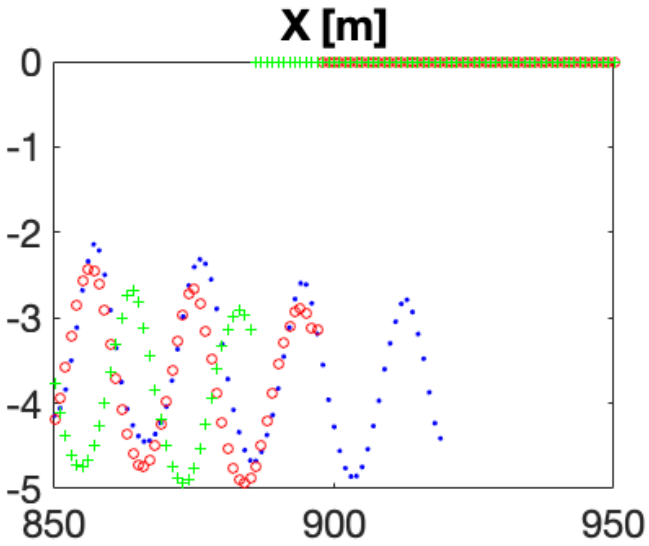

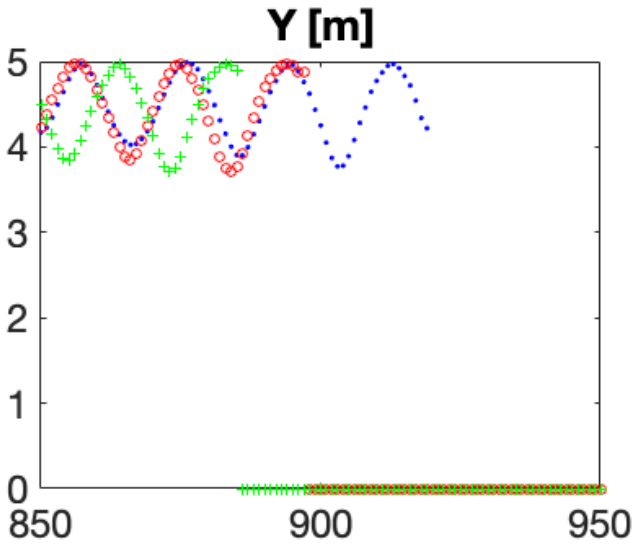

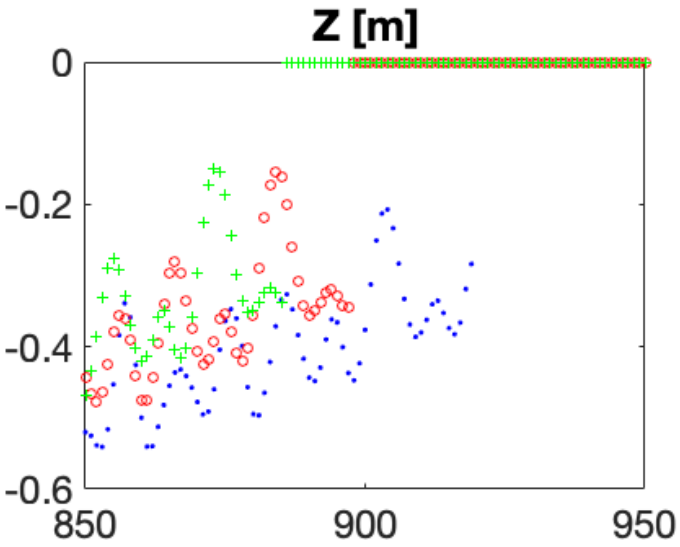

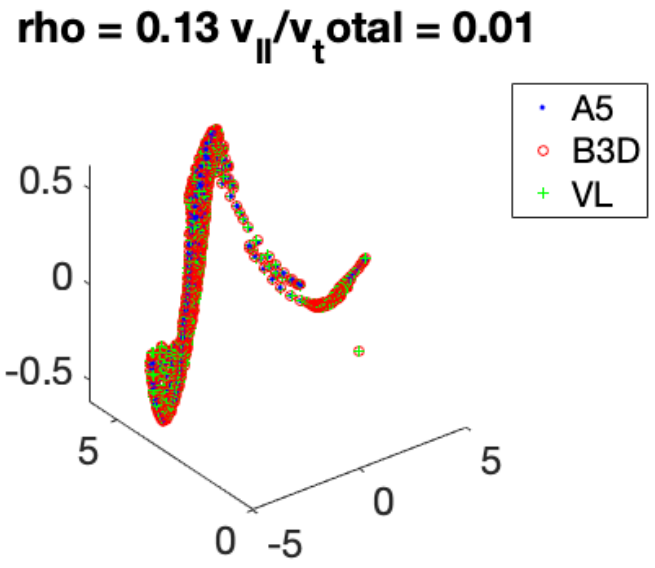

Strongly passing particles show generally good agreement

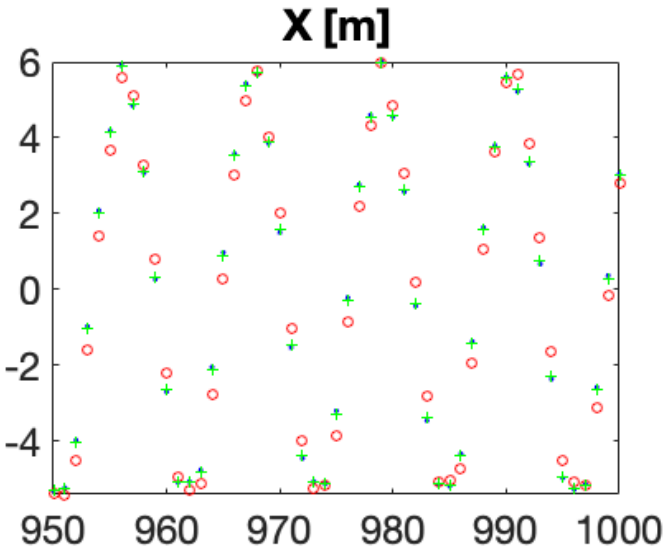

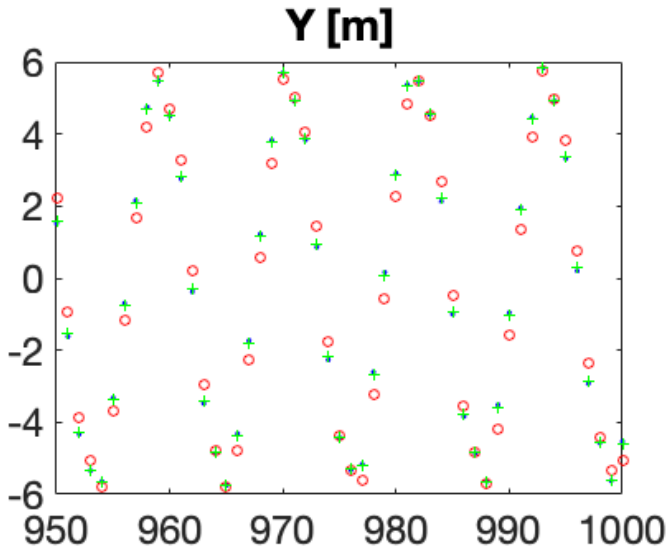

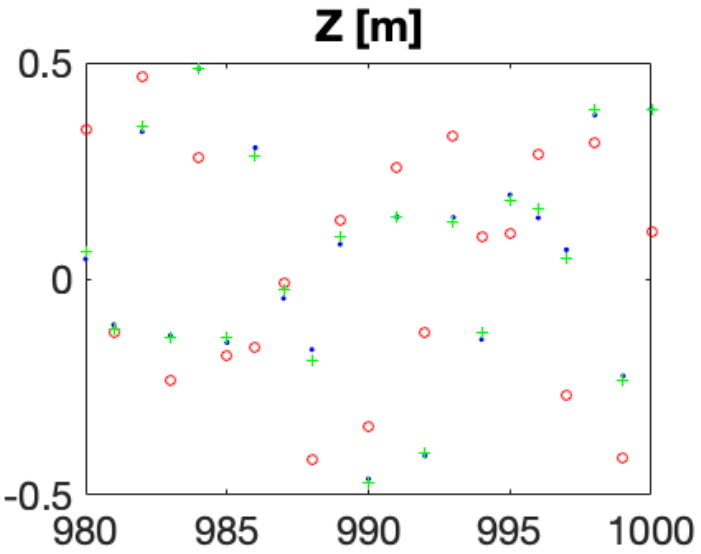

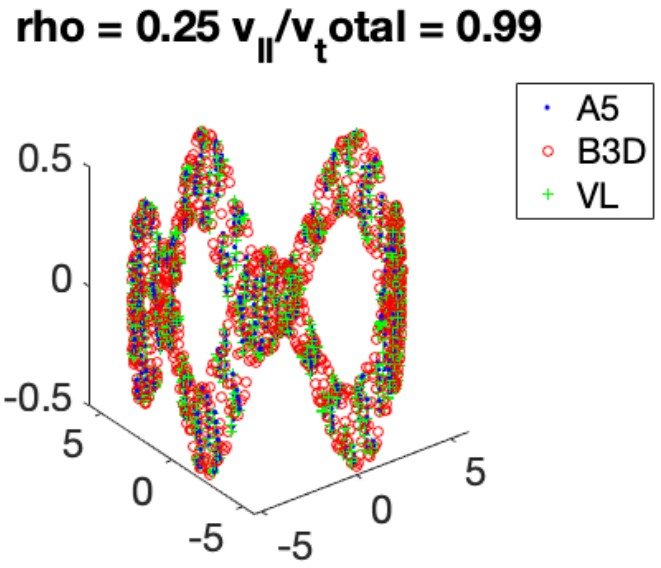

Validation of ASCOT5 has not been successful

- ASCOT5 fails to reproduce toy model analytic result.